Probing positivity at the LHC with exclusive photon-fusion processes

Jiayin Gu [a,b] **and Chi Shu** [a,c]

ᵃDepartment of Physics and Center for Field Theory and Particle Physics, Fudan University,
2005 Song Hu Road, Shanghai 200438, China

ᵇKey Laboratory of Nuclear Physics and Ion-beam Application (MOE), Fudan University,
220 Handan Road, Shanghai 200433, China

ᶜDepartment of Physics and Enrico Fermi Institute, University of Chicago,
5640 S Ellis Ave., Chicago, IL 60637, U.S.A.

E-mail: jiayin_gu@fudan.edu.cn, cshu20@fudan.edu.cn

ABSTRACT: By tagging one or two intact protons in the forward direction, it is possible to select and measure exclusive photon-fusion processes at the LHC. The same processes can also be measured in heavy ion collisions, and are often denoted as ultraperipheral collisions (UPC) processes. Such measurements open up the possibility of probing certain dimension-8 operators and their positivity bounds at the LHC. As a demonstration, we perform a phenomenological study on the $\gamma\gamma \to \ell^+\ell^-$ processes, and find out that the measurements of this process at the HL-LHC provide reaches on a set of dimension-8 operator coefficients that are comparable to the ones at future lepton colliders. We also point out that the $\gamma q \to \gamma q$ process could potentially have better reaches on similar types of operators due to its larger cross section, but a more detailed experimental study is need to estimate the signal and background rates of this process. The validity of effective field theory (EFT) and the robustness of the positivity interpretation are also discussed.

https://doi.org/10.1007/JHEP05(2024)183

Contents

1   Introduction

Probing dimension-8 (dim-8) operators of the Standard Model Effective Field Theory (SMEFT) at the Large Hadron Collider (LHC) is both an interesting and a challenging task. Certain dim-8 operators are subject to the so-called positivity bounds, assuming the underlying UV physics is consistent with the fundamental principles of quantum field theory (QFT), including unitarity, locality, analyticity and Lorentz invariance [1–27]. Such positivity bounds do not exist for dim-6 operators without additional assumptions [28–36]. On the other hand, dim-6 operators are generally expected to provide the leading new physics contributions, assuming the scale of new physics is sufficiently higher than the energy scale of the collider so that the EFT expansion is valid in the first place. This creates a conundrum for probing dim-8 operators and their positivity bounds at the LHC. On the one hand, due to their energy enhancements ($\sim E^4$) we want to make use of the high energy events to maximize the sensitivity and to discriminate them from the dim-6 effects; on the other hand, high energy events typically have low statistics, and are poorly measured. This leads to issues in the EFT interpretation, as the reach on the new physics scale Λ tend to be comparable or even lower than the center-of-mass energy of the events. Furthermore, in these cases the dim-8-squared contribution can also be sizable. Probing positivity bounds requires us to measure the interference term between SM and the dim-8 contribution, which is sensitive to the signs of the Wilson coefficients. While a sizable dim-8-squared contribution can be considered as an important signal for new physics (putting aside the EFT validity problem), it is effectively a background for probing positivity. Several studies pointed out the advantages of future lepton colliders in probing the dim-8 operators and positivity bounds [12, 14, 37, 38].[1] In general, the high precision measurements that can be achieved at future lepton colliders makes the EFT interpretation more robust, and the interference terms between SM and the dim-8 contribution dominate over the dim-8 square terms. It was also pointed out in [14] that the

---

[1]For comparisons with the reaches of similar processes at hadron colliders, see e.g. refs. [39–41].

leading dim-6 contribution is strongly suppressed in the process $e^+e^- \to \gamma\gamma$ (or $\mu^+\mu^- \to \gamma\gamma$), so the measurement of its cross section provides a direct probe of the positivity bounds of the corresponding dim-8 operators. However, none of the proposed future lepton collider projects has been approved and their timelines are still unclear at the current moment.

In recent years, both ATLAS and CMS experiments have measured exclusive photon-fusion processes, including $\gamma\gamma \to \ell^+\ell^-$, $\tau^+\tau^-$, $\gamma\gamma$, W^+W^-, ZZ, and $\pi^+\pi^-$ [42–47]. Crucially, these photon-fusion processes are identified by requiring at least one intact forward protons, which can be measured with the ATLAS forward proton tagger (AFP) [48, 49] or the TOTEM detector at CMS [50]. Similar processes have also been measured and extensively studied in heavy ion collision experiments with forward nucleus taggers, and are often denoted as ultraperipheral collisions (UPC) processes [51–56]. The proton tagging also significantly reduces QCD background, as those would not leave the proton intact. In particular, the reverse of the process $e^+e^-(\mu^+\mu^-) \to \gamma\gamma$, $\gamma\gamma \to \ell^+\ell^-$, is a very clean channel at the LHC, probes the same set of operators as $e^+e^-(\mu^+\mu^-) \to \gamma\gamma$ while also benefits from a suppressed dim-6 contribution. It thus provides an alternative to the measurements at future lepton colliders.[2] The $\gamma\gamma \to \ell^+\ell^-$ process has several clear advantages compared with the fusion processes of the weak gauge bosons. First, the leading contributions to the $WW \to \ell^+\ell^-$ or $WZ/\gamma \to \ell\nu$ process comes from the dim-6 operators. Second, with massive gauge bosons, other dim-8 operators (in addition to the ones in equation (A.4)) with different helicity structures also contribute to the interference term with the SM. The presence of dim-6 and dim-8 contributions with different helicity structures makes the interpretation of positivity bounds much more complicated. Finally, without the proton tagging, the weak gauge boson fusion processes also suffer more from QCD backgrounds. Other photon-fusion processes can also be exploited to probe dim-8 operators and positivity bounds.

In this paper, we perform a phenomenological study to demonstrate the physics potential of the $\gamma\gamma \to \ell^+\ell^-$ channel in probing dim-8 operators and their positivity bounds. We calculate the parton-level differential cross section in $\gamma\gamma \to \ell^+\ell^-$ and use the effective photon parton distribution function (PDF) in ref. [61] to obtain the full differential cross section. By a comparison with the ATLAS $\gamma\gamma \to \ell^+\ell^-$ analysis [43], we apply a proton tagging efficiency to our results and then scale the luminosity to obtain the projection of this measurement after the entire HL-LHC. We find that, while the future lepton colliders still provide better reaches on the corresponding dim-8 operator coefficients, the reach of the HL-LHC is comparable and within the same order. However, at the LHC the reach on the new physics scale (Λ_8) is comparable to the maximum invariant mass of the lepton pairs, $m_{\ell\ell}$. An upper cut on $m_{\ell\ell}$, while reducing the reach on Λ_8, improves the situation of EFT validity to some extent. On the other hand, we have checked that the dim-8 squared contributions (which are formally at the same order as the interference of SM and dim-12 operators) have relatively small effects compared with the interference term. We apply the same methods to the $\gamma q \to \gamma q$ process, which probes a similar set of dim-8 operators, with leptons replaced by quarks. Due to the large quark PDF (which however could be different from the conventional quark PDF for this kind of semi-dissipative process), this process has a much larger cross section, leading to a potentially much better reach on the operator coefficients, as well as a more robust EFT

---

[2]This process is also of high theoretical interests in other aspects. See e.g. refs. [57–60].

interpretation. However, a detailed experimental study is needed to estimate the background of this channel before such a claim can be made.

The rest of this paper is organized as follows. In section 2, we lay out the theoretical framework of the $\gamma\gamma \to \ell^+\ell^-$ processes, the treatment of the effective photon PDF before doing a collider analysis to obtain the projection of this measurement at the HL-LHC. The analysis on $\gamma q \to \gamma q$ is presented in section 3. We conclude in section 4 with a discussion on other possible measurements of dim-8 operators with the forward proton/nucleus tagger. More details on the dim-8 operators in $\gamma\gamma \to \ell^+\ell^-$ and their positivity bounds are provided in appendix A.

2 The $\gamma\gamma \to \ell^+\ell^-$ process

2.1 The parton-level process and positivity bounds

It was shown in ref. [14] that the leading new physics contribution in the $e^+e^- \to \gamma\gamma$ process comes from dim-8 operators. This is due to several reasons: first, the tree-level SM amplitude has only one helicity configuration, where the two fermions (and the two photons) have opposite helicities. One insertion of the dim-6 dipole operator generates a different helicity amplitude that does not interfere with the leading SM amplitude. Second, two insertions of dipole operators, formally at the dim-8 level, can be safely neglected due to the strong constraints from low energy experiments [62–65]. Third, while many dim-6 operators contribute at the one-loop level, they generally contribute at the tree level to other EW processes that are measured with a similar or even better precision. If those experimental constraints are considered, one could safely ignore the one-loop contributions in the $e^+e^- \to \gamma\gamma$ process.

Due to crossing symmetry, similar arguments also apply to the $\gamma\gamma \to \ell^+\ell^-$ processes, except in this case one does not have a future lepton collider to constrain some of the dim-6 operators that could enter $\gamma\gamma \to \ell^+\ell^-$ at the one-loop level. Nevertheless, many of these can be probed at the LHC as well. In particular, the anomalous triple gauge coupling λ_Z (corresponding to the operator $\mathcal{O}_{3W} = \frac{1}{3!} g \epsilon_{abc} W_\mu^{a\,\nu} W_{\nu\rho}^b W^{c\,\rho\mu}$) can be constrained at the level of 10^{-3} with the diboson measurements at the HL-LHC [66, 67]. Combined with the constraints from LEP, the third argument above still generally holds. The crossing symmetry also implies that we could directly infer from the results in ref. [14] to obtain (for one lepton generation)

$$\frac{\mathrm{d}\sigma\left(\gamma\gamma \to \ell^+\ell^-\right)}{\mathrm{d}|\cos\theta|} = \frac{e^4}{8\pi s} \left[\frac{1 + c_\theta^2}{1 - c_\theta^2} + \left(a_L + a_R\right) \frac{s^2 \left(1 + c_\theta^2\right)}{8e^2 v^4} \right], \qquad (2.1)$$

where $c_\theta \equiv \cos\theta$, θ is the production polar angle, s is the Mandelstam variable, a_L (a_R) is the coefficients of the $\gamma\gamma\bar{e}_L e_L$ ($\gamma\gamma\bar{e}_R e_R$) dim-8 contact interaction. The definitions of a_L and a_R and their connections with the dim-8 operator coefficients are provided in appendix A. Note that we have summed over the final state polarizations of the leptons in equation (2.1). In this case, the experiment is only sensitive to the combination $a_L + a_R$. The positivity bounds are simply

$$a_L \geq 0, \qquad a_R \geq 0, \qquad (2.2)$$

which implies that

$$\frac{d\sigma}{d|\cos\theta|}(\gamma\gamma \to \ell^+\ell^-) \geq \frac{d\sigma_{\text{SM}}}{d|\cos\theta|}(\gamma\gamma \to \ell^+\ell^-)\,. \qquad (2.3)$$

In principle, the positivity bound applies to all fermion-pair final states, including also $\gamma\gamma \to q\bar{q}$. We focus on the leptonic final states, e^+e^- and $\mu^+\mu^-$, to avoid a potential large QCD background. It should be noted that for $\gamma\gamma \to \tau^+\tau^-$, if the final state tau polarization can be measured, one could in principle discriminate the effects of a_L and a_R and separately constrain them. We leave a detailed analysis of the $\gamma\gamma \to \tau^+\tau^-$ channel to future studies.

2.2 The $pp \to p\,\ell^+\ell^-\,p$ process with effective photon PDF

An automated generation tool for exclusive photon fusion processes was developed in ref. [61]. It implements the Equivalent Photon Approximation (EPA), and calculates the cross sections using photon flux derived from electric dipole and charge form factors. Ref. [61] essentially provides an effective photon PDF[3] for proton and nuclear collisions at any energy. Using the results in ref. [61], we convolute the parton-level cross section of equation (2.1) to the proton/nucleus level with two general nuclei A and B,

$$\frac{d\sigma\left(AB \to A\left(\gamma\gamma \to l^+l^-\right)B\right)}{d|\cos\theta|} = \int \frac{dE_{\gamma_1}}{E_{\gamma_1}} \frac{dE_{\gamma_2}}{E_{\gamma_2}} \frac{\mathrm{d}^2 N^{(\text{AB})}_{\gamma_1/\text{Z}_1,\gamma_2/\text{Z}_2}}{\mathrm{d}E_{\gamma_1}\,\mathrm{d}E_{\gamma_2}} \frac{d\sigma\left(\gamma\gamma \to l^+l^-\right)}{d|\cos\theta|}\,, \qquad (2.4)$$

where

$$\frac{\mathrm{d}^2 N^{(\text{AB})}_{\gamma_1/\text{Z}_1,\gamma_2/\text{Z}_2}}{\mathrm{d}E_{\gamma_1}\,\mathrm{d}E_{\gamma_2}} = \int \mathrm{d}^2\boldsymbol{b}_1\,\mathrm{d}^2\boldsymbol{b}_2 P_{\text{no inel}}\,\left(|\boldsymbol{b}_1 - \boldsymbol{b}_2|\right) N_{\gamma_1/\text{Z}_1}\left(E_{\gamma_1},\boldsymbol{b}_1\right) N_{\gamma_2/\text{Z}_2}\left(E_{\gamma_2},\boldsymbol{b}_2\right)$$
$$\times \theta\left(b_1 - \epsilon R_{\text{A}}\right)\theta\left(b_2 - \epsilon R_{\text{B}}\right)\,. \qquad (2.5)$$

In the expression, the step function $\theta\left(b - \epsilon R\right)$ enforces a constraint on the impact range, characterized by the impact parameter b, the nuclear radius R as well as the positive parameter ϵ. Typically, in the Electric Dipole Form Factor (EDFF) method, ϵ is set to 1. Additionally, $P_{\text{no inel}}\,(b)$ denotes the probability of having no inelastic hadronic interaction. For simplicity, we take a reasonable approximation $P_{\text{no inel}}\,(b) = 1$, implying a 100% the survival rate. As demonstrated in ref. [61], this approximation does not significantly affect the outcomes for p-p collisions. The term $N_{\gamma_1/\text{Z}_1}\left(E_{\gamma_1},\boldsymbol{b}_1\right)$ describes the photon number density, derived by EDFF method:

$$N^{\text{EDFF}}_{\gamma/\text{Z}}\left(E_\gamma,b\right) = \frac{Z^2\alpha}{\pi^2}\frac{\xi^2}{b^2}\left[K_1^2(\xi) + \frac{1}{\gamma_\text{L}^2}K_0^2(\xi)\right]\,, \qquad (2.6)$$

where Z is the number of protons in the nucleus, $\xi = E_\gamma b/\gamma_\text{L}$, and K_i represents modified Bessel functions. The parameter α is the fine structure constant, while Z is the nuclear charge. For proton collisions, one simply sets $Z = 1$ and $R_A = R_B = R_{\text{proton}}$.

The cross section of $\gamma\gamma$ fusion processes obtained with the effective photon PDF are generally associated with a theoretical uncertainty of $\mathcal{O}(10\%)$ [61]. Furthermore, the effective

---

[3]Strictly speaking, the term "PDF" is inaccurate since the proton remains intact.

photon PDF explicitly assumes that the photon has zero transverse momentum, and also ignores possible polarizations of the photon. These effects have important impacts for the study of UPC processes at low energies [58, 60, 68–72], but they have much smaller effects at the high energy region ($\gtrsim 100\,\text{GeV}$) that we focus on in our study.

2.3 Collider reach

With the full differential cross section in equation (2.4), we are now ready to perform a collider study to obtain the precision reach on the a_L and a_R parameters at the HL-LHC. To estimate the selection efficiency, we use MadGraph5 [73] with the built-in photon PDF package from ref. [61] to generate $pp \to p\,\ell^+\ell^-\,p$ events. We then apply the main selection cuts in ref. [43]. First, each lepton is required to have $p_T > 15\,\text{GeV}$ and $\eta < 2.5$ — these cuts do not have a significant impact on the signal events, as we checked that the signal cross section only reduced by 3% compared with the MadGraph default cuts. We then require the invariant mass of the lepton pair $m_{\ell\ell}$ to be larger than $105\,\text{GeV}$ to avoid Z backgrounds. The events with lower invariant mass are also less useful for our analysis due to the large energy enhancements of dim-8 effects. After these basic cuts, we compare the cross section of the simulated events with the reported one in ref. [43]. The ratio between them provides a simple estimation of the selection efficiency of the forward proton tagger, which we find to be around 11%. We compare the invariant mass distribution $m_{\ell\ell}$ and found a reasonable agreement between the simulation after applying the 11% efficiency. We also note from ref. [43] that the background in the $pp \to p\,\ell^+\ell^-\,p$ channel is much smaller than the signal after the selection cuts, so we will simply ignore the background in our study.

After the comparison with ref. [43], we then scale the luminosity to the HL-LHC projection (two detectors, each with $3\,\text{ab}^{-1}$) and perform a simple χ^2 analysis to extract the reach on a_L and a_R. As mentioned above, a universal proton-tagging efficiency of 11% is applied. Different from the lepton collider case which has a fixed center-of-mass energy, here we have a distribution for the center-of-mass energy (or the invariant mass of the lepton pair, $m_{\ell\ell}$), which contains crucial information. To extract it, we perform a binned analysis, dividing $m_{\ell\ell} \in [105, 1500]\,\text{GeV}$ into 14 bins with a bin width of $100\,\text{GeV}$ (except the first bin which is $95\,\text{GeV}$ wide). A χ^2 is constructed for each bin based on the statistical uncertainty of the fiducial cross section, which are combined (assuming no correlation among different bins) to form the total χ^2.

The $\Delta\chi^2 = 1$ contour is shown in figure 1 for the projected HL-LHC pp run with a total luminosity of $2 \times 3\,\text{ab}^{-1}$. We have imposed an upper bound of $1.5\,\text{TeV}$ on the maximal value of $m_{\ell\ell}$. For comparison, we also shown the bounds from the $e^+e^- \to \gamma\gamma$ measurement at the $240\,\text{GeV}$ run of CEPC [74] and FCC-ee [75] and the $250\,\text{GeV}$ run of ILC [76], reproduced from ref. [14] with updated run scenario for the CEPC [77]. The difference between CEPC and FCC-ee is due to their different luminosities, which is $20\,\text{ab}^{-1}$ for CEPC-240 GeV and $5\,\text{ab}^{-1}$ for FCC-240 GeV according to the current projections. As pointed out in ref. [14], without the knowledge of the polarization (or helicity) of the initial or final state particles, only the combination $a_L + a_R$ can be constrained. This is the case for CEPC and FCC-ee, and HL-LHC as well. We find that the (1-sigma) precision on $a_L + a_R$ could reach around 7.3×10^{-4} at the HL-LHC, which is about a factor of 3 worse than the one of FCC-ee.
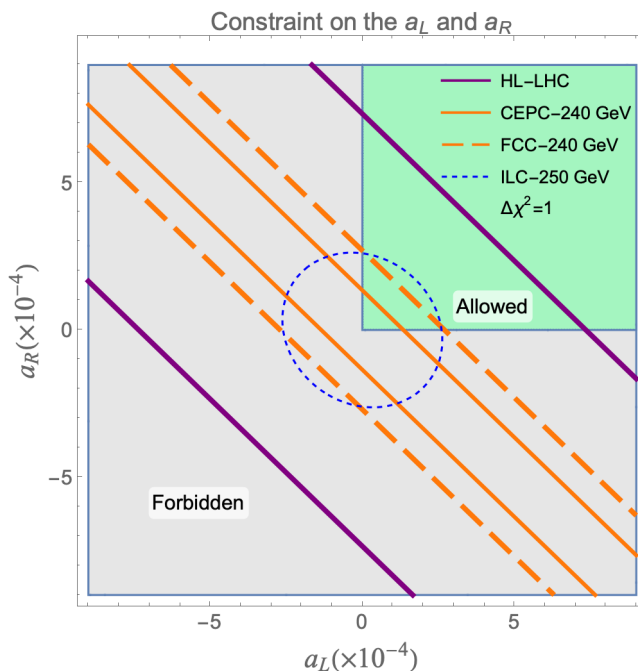
Figure 1. The projected precision reach on the a_L and a_R from the $\gamma\gamma \to \ell^+\ell^-$ measurement at HL-LHC and the $e^+e^- \to \gamma\gamma$ measurements at future lepton colliders. For the latter, the results are reproduced from ref. [14] but with updated CEPC 240 GeV luminosity $(20\,\mathrm{ab}^{-1})$. Only the green area is allowed by positivity bounds. Note that without beam polarization or other means to separate different initial or final helicity states, only the combination $a_L + a_R$ can be constrained. For the $\gamma\gamma \to \ell^+\ell^-$ measurement, a maximum value of $1.5\,\mathrm{TeV}$ is imposed on the invariant mass of the lepton pair, $m_{\ell\ell}$.

As mentioned above, the large center-of-mass energy $(m_{\ell\ell})$ at the LHC raises the question on the validity of EFT. One way to quantitatively address this problem is to impose an upper cut on $m_{\ell\ell}$ and compare it with the scale of new physics that can be reached from the analysis, which requires assumptions on the coupling strength [78]. Assuming a coupling of order one, We take a naïve definition of the new physics scale, $\Lambda_8 \equiv v/a^{1/4}$ where $a = a_L + a_R$,[4] and examine how the 95% confidence-level (C.L.) reach on Λ_8 changes for different choices of upper bounds on $m_{\ell\ell}$ (which we denote as $\sqrt{s}_{\max}$). Our results are shown in figure 2. For better visualization, we have shown both Λ_8 (left panel) and $\Lambda_8/\sqrt{s}_{\max}$ (right panel), while the dotted line corresponds to $\Lambda_8 = \sqrt{s}_{\max}$ in both panels. As we can see, with our default cut $m_{\ell\ell} < 1.5\,\mathrm{TeV}$, the Λ_8 that can be reached is comparable with $\sqrt{s}_{\max}$. A smaller $\sqrt{s}_{\max}$ improves $\Lambda_8/\sqrt{s}_{\max}$, but also worsen the reach on Λ_8.

So far, our analysis only considers dim-8 contributions via their interference with the SM. The impacts of the dim-8 squared terms are shown in figure 3. The square terms may also be considered as an theory error from missing higher order contributions [79], but one should note that the dim-8 squared terms are of the order Λ^{-8}, while the dim-10 operators are at Λ^{-6}. The results are shown for 3 choices of $\sqrt{s}_{\max}$, 500 GeV (left panel), 1000 GeV

---

[4]More explicitly, one could write the Wilson coefficient as $\frac{c_8}{\Lambda_8^4} \equiv \frac{a}{v^4}$, where c_8 is a dimensionless coupling strength. Setting $c_8 = 1$ gives $\Lambda_8 = v/a^{1/4}$.
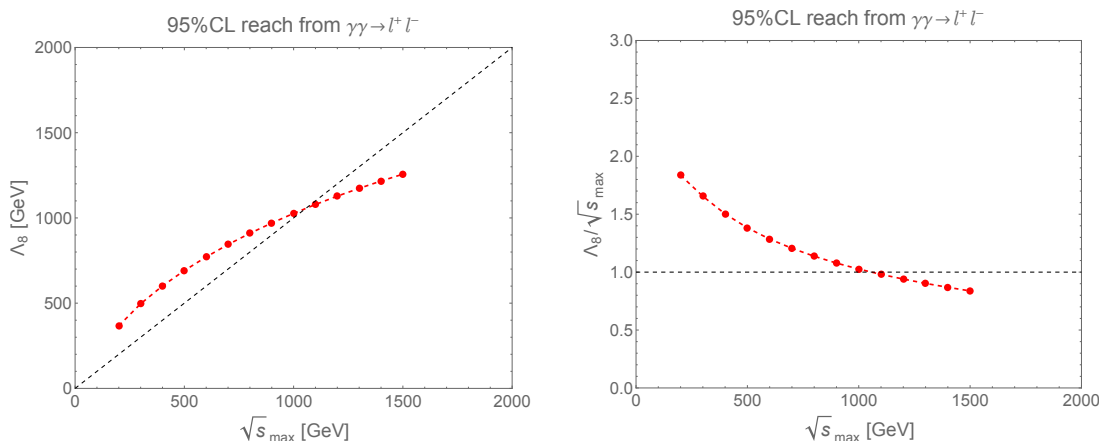
Figure 2. *Left*: the 95% C.L. reach on $\Lambda_8 \equiv v/a^{1/4}$ from the $\gamma\gamma \to \ell^+\ell^-$ measurement at HL-LHC as a function of the upper bound of the lepton-pair invariant mass, $\sqrt{s}_{\text{max}}$. *Right*: the same result shown in terms of $\Lambda_8/\sqrt{s}_{\text{max}}$. The dotted line corresponds to $\Lambda_8 = \sqrt{s}_{\text{max}}$ in both panels.
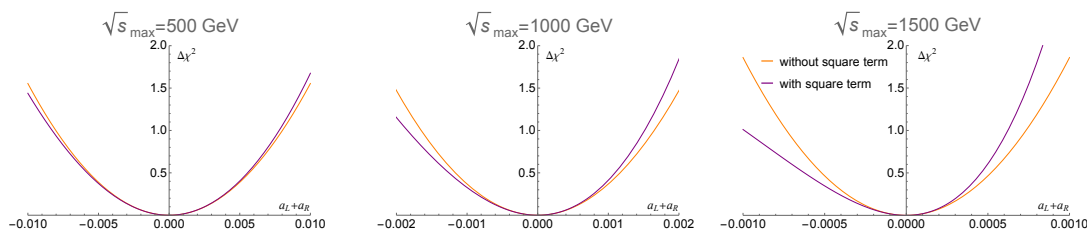

Figure 3. The $\Delta\chi^2$ as a function of $a = a_L + a_R$ from the $\gamma\gamma \to \ell^+\ell^-$ measurement at HL-LHC, without (orange) or with (purple) the dim-8 squared terms. The results are shown for 3 choices of $\sqrt{s}_{\text{max}}$ (maximum invariant mass of the lepton pair), 500 GeV (left), 1000 GeV (middle) and 1500 GeV (right).

(middle panel) and 1500 GeV (right panel). In each case, we show the $\Delta\chi^2$ as a function of $a = a_L + a_R$ both without and with the dim-8 squared terms. We see that, even for $\sqrt{s}_{\text{max}} = 1500$ GeV, the impact of the dim-8 square terms is relatively small, which changes the 1-sigma bound on a from $\pm 7.3 \times 10^{-4}$ to $[-9.9, 6.2] \times 10^{-4}$.

As mentioned above, the statement on the EFT validity depends on the coupling strength of the underlying theory. If a strongly coupled theory is assumed (e.g., as in ref. [3]), one typically has $c_8 \gg 1$, in which case the reach on Λ_8 is significantly larger than what we have obtained assuming $c_8 = 1$. Correspondingly, the dim-12 contribution ($\sim c_{12}/\Lambda$) is suppressed compared with the dim-8 squared contribution ($\sim c_8^2/\Lambda$) since $c_8^2 \gg c_{12}$. In such cases, a more robust interpretation of the experimental result as a test of positivity bounds can be made.

We repeat the same analysis for the Pb-Pb collision experiment at HL-LHC. The cross section of the UPC process has a large enhancement proportional to Z^4, as Z is also the electric charge of the nucleus. However, the heavy ion collision runs generally have much smaller luminosities, while the PDF of photon also drops significantly faster at large x [61]. Assuming a center-of-mass energy of 14 TeV and a total luminosity of $40 \, \text{nb}^{-1}$ (which roughly corresponds to the total integrated luminosity at the end of Run 4 [80]), even with a 100%

System	$\sqrt{s}$	Luminosity	Radius	1σ bound on $a_L + a_R$
Pb-Pb	14 TeV	$40\,\text{nb}^{-1}$	7.1 fm	~ 0.1

Table 1. The result of the $\gamma\gamma \to \ell^+\ell^-$ measurement in Pb-Pb collision at HL-LHC. We assume a total luminosity of $40\,\text{nb}^{-1}$, a 100% signal selection efficiency and $P_{\text{no inel}} = 1$. A maximum value of $1.5\,\text{TeV}$ is imposed on the invariant mass of the lepton pair.

tagging efficiency and $P_{\text{no inel}} = 1$, we find that the reach on $a_L + a_R$ is only at the 10^{-1} level, which is significantly worse than the projected HL-LHC *pp* run result. The result is summarized in table 1.

3 The $\gamma q \to \gamma q$ process

Similar to the $\gamma\gamma \to \ell^+\ell^-$ process, the hadronic process, $\gamma\gamma \to q\bar{q}$, can also be measured and is sensitive to a set of dim-8 operators involving quarks, which are subject to positivity bounds as well. However, it may suffer from a large QCD background and it is not clear whether a meaningful sensitivity could be reached (except maybe the $b\bar{b}$ case for which b-tagging could be exploited). On the other hand, the process $\gamma q \to \gamma q$ is sensitive to the same set of operators, and may provide better sensitivities. To the best of our knowledge, it has not been measured so far. This process has two advantages: first, the final state photon could be used to reduce QCD backgrounds; second, the initial state quark has a larger PDF than photon, so the cross section of this process is larger, especially at high energies. A proper estimation of backgrounds of this process is beyond the scope of this paper. As a proof of principle, here we perform an ideal signal-only analysis to estimate the best-possible reach of this channel. We also note that $\gamma q \to \gamma q$ is also related to $q\bar{q} \to \gamma\gamma$ by crossing, while the latter could benefit from an even larger event rate. The measurement of the $q\bar{q} \to \gamma\gamma$ process provides important and complementary probes to the dim-8 operators and their positivity bounds [81].

The $\gamma q \to \gamma q$ amplitude is related to the $\gamma\gamma \to q\bar{q}$ one by a $s \leftrightarrow t$ crossing, The parton level differential cross section is given by

$$\frac{\mathrm{d}\sigma\,(\gamma q \to \gamma q)}{\mathrm{d}\cos\theta} = \frac{Q^4 e^4}{16\pi s}\left[\frac{2}{1+c_\theta} - (a_L + a_R)\,\frac{s^2}{2Q^2 e^2 v^4}\right], \tag{3.1}$$

where Q is the charge of q. Here, from the proton tagger we know which side the photon comes from, and the two final states are also distinguishable, so the sign of $\cos\theta$ is measurable. Note that, due to crossing, now the interference term is destructive, and the positivity bounds $a_L, a_R \geq 0$ implies that

$$\frac{d\sigma}{d\cos\theta}(\gamma q \to \gamma q) \leq \frac{d\sigma_{\text{SM}}}{d\cos\theta}(\gamma q \to \gamma q)\,. \tag{3.2}$$

We convolute equation (3.1) with the "photon PDF" in subsection 2.2 and the quark PDF to obtain the hadron-level cross section. Again, here the "photon PDF" is an inaccurate term since the proton needs to be intact for the event to be selected by the forward proton tagger. The proton that produces a quark, on the other hand, needs to be explicitly
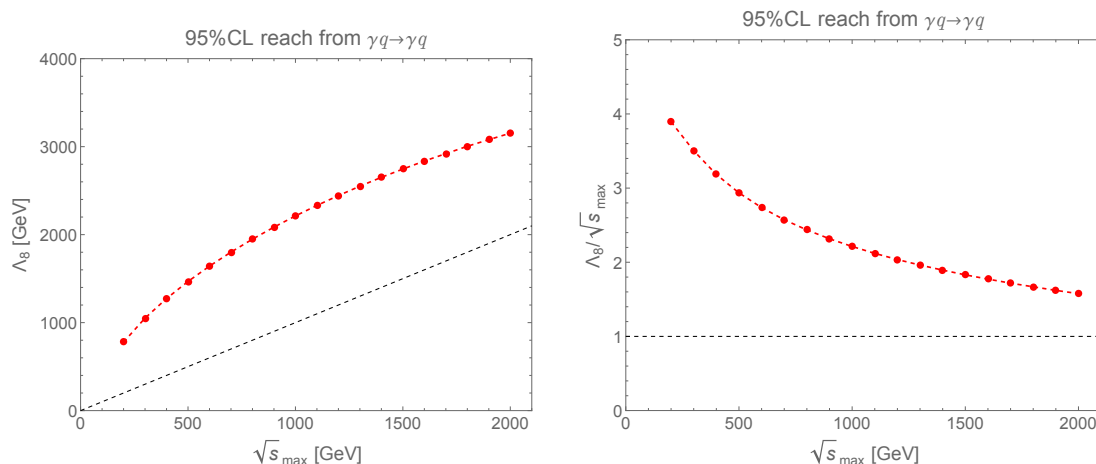
Figure 4. Same as figure 2 but for $\gamma q \to \gamma q$. a_L and a_R are assumed to be universal for all quark flavors.

broken. It is unclear what the rate of such an "semi-dissipative" process is, and whether the conventional quark PDF would provide a reasonable approximation.[5] Needless to say, the precise estimation of the SM rate of this process is crucial for the study of the dim-8 contribution, but is beyond the scope of this paper. For simplicity, here we use the MMHT quark PDF [84]. We also assume that the proton tagging efficiency to be 5.5%, half of the 11% of the $\gamma\gamma \to \ell^+\ell^-$ process.[6]

It is generally difficult to tag the final state quark flavor (except for the b quark). Here we make a simple assumption that $a = a_L + a_R$ are universal for all quark flavors, and use the inclusive semi-dissipative process $pp \to p\gamma j + X$ to constrain a. We assume statistical uncertainties only and impose a upper bound ($\sqrt{s}_{\max}$) of 1.5 TeV on the γ-jet pair invariant mass. After performing a χ^2 analysis with binned invariant mass distribution (similar to the one of $\gamma\gamma \to \ell^+\ell^-$), we obtain a 1-sigma bound of $\pm 1.8 \times 10^{-5}$ for the a parameter of quark operators. The results are also shown in figure 4 in terms of the 95% C.L. reach on $\Lambda_8 \equiv v/a^{1/4}$ as a function of $\sqrt{s}_{\max}$. Compared with the same result for $\gamma\gamma \to \ell^+\ell^-$ in figure 2, we see that a significantly larger Λ_8 can be reached for the $\gamma q \to \gamma q$ channel, which is in the range of several TeVs. This also improves the robustness of the EFT validity, as a large value (> 2) of $\Lambda_8/\sqrt{s}_{\max}$ can be achieved without a strict choice of $\sqrt{s}_{\max}$. It is also possible to pick out the $\gamma b \to \gamma b$ process with b-tagging and probe the positivity bounds of the operator involving bottom quarks. Assuming a 50% b-tagging rate, we obtain a one-sigma bound of $\pm 2.0 \times 10^{-4}$ for the a parameter of the bottom-quark operators.

We note again that the result of the $\gamma q \to \gamma q$ channel could receive a significant impact from potential backgrounds. With large QCD background, even a tiny mistagging rate (that

---

[5]The $\gamma q \to \gamma q$ process can also be produced with the real photon PDF [82], but the signal selection can be extremely challenging without the proton tagger. On the other hand, there is a diffractive quark parton distribution function [83] that leaves the proton intact, but it is unclear whether it is relevant at high energy.

[6]This assumes the proton tagger is only on one-side of the detector, and the tagging efficiency is independent of the process. If there are proton taggers on both sides, one would instead conclude from the comparison with ref. [43] that each tagger has an efficiency of $1 - \sqrt{1 - 11\%} \approx 5.7\%$, which is the tagging efficiency of the $\gamma q \to \gamma q$ process. Numerically this makes very little difference.

a $pp \to \gamma j$ event is somehow mistagged by the forward proton tagger) could result in an overwhelming amount of backgrounds. An experimental study for background estimation is thus crucial for this channel. A naive estimation using MadGraph5 suggests that the cross section of $pp \to \gamma j$, when applied the same selection cuts[7] (except the proton tagging), is of order $\sim 10^4$ pb, while $\gamma q \to \gamma q$ is around 2 pb after the proton tagging selection. This suggests that the mistagging rate for the proton tagger to mistakenly select $pp \to \gamma j$ needs to be around or below 10^{-4} in order to reduce the background statistics to the same level as the signal one. In addition, the process $\gamma g \to \gamma g$, while loop-suppressed in the SM, also contributes to the same channel. Due to its different helicity structure, an angular distribution analysis will be very useful in removing this background or distinguishing the dim-8 contributions in it from the ones in $\gamma q \to \gamma q$. It should also be noted that the dim-6 squared contribution from quark dipoles also contribute to the $\gamma q \to \gamma q$ processes, and unlike $\gamma\gamma \to \ell^+\ell^-$, the quark dipole operators are much less constrained. Since their contributions to the amplitude scales as $v^2 E^2$, it is possible to distinguish their effects from the ones of $a_{L,R}$ by their different energy dependence. We refer the readers to ref. [81] for a more detailed analysis of the impacts of the gluon process and the dim-6-squared contributions.

4   Conclusion

In this paper, we have performed a simple collider analysis of the $\gamma\gamma \to \ell^+\ell^-$ process to estimate projected reaches on the corresponding dim-8 operator coefficients at the HL-LHC. The dim-8 operator coefficients are subject to positivity bounds, making them of high theoretical interests. For pp collisions, we found a reach of $\sim 10^{-4}$ in the effective coupling combination $a_L + a_R$ of the contact $\gamma\gamma\ell^+\ell^-$ interactions, which naïvely (assuming couplings of order one) translates to a 95% C.L. reach on the new physics scale Λ_8 of ~ 1 TeV. The reaches are comparable to (but slightly worse than) the ones at future lepton colliders. Furthermore, having fermions in the final state means that it is easier to probe operators of different flavors, while for lepton colliders the initial state fermions are fixed by the collider beams. For heavy ion collisions, a much lower reach was found despite an enhancement from the large nucleus electric charge. This is due to both a smaller luminosity and a smaller parton-level center-of-mass energy. Careful treatments are needed to ensure the validity of the EFT expansion, at least to a reasonable level. For $\gamma\gamma \to \ell^+\ell^-$, the new physic scale that can be reached turns out to be comparable with the maximum center-of-mass energy of the lepton pair. On the other hand, we found the dim-8 squared contribution to have a relatively small impact. Overall, the $e^+e^- (\mu^+\mu^-) \to \gamma\gamma$ measurements at future lepton colliders still have advantages in a more robust EFT interpretation, which is important for testing positivity bounds.

We also performed a similar analysis for $\gamma q \to \gamma q$ in pp collision with the simple assumption of a conventional quark PDF and no backgrounds. The reach is significantly better, with precision of $\sim 10^{-5}$ for $a_L + a_R$ (assuming the operator coefficients are universal for all quark flavors) and a reach on Λ_8 of about $2 \sim 4$ TeV. For $\gamma q \to \gamma q$, we also found that a sufficiently large ratio ($\gtrsim 2$) between the new physic scale that can be reached (assuming

---

[7]This includes a minimum invariant mass cut of 100 GeV for the γj pair. Above 100 GeV we also find the signal and background invariant mass distributions to be somewhat similar, so a more stringent cut does not help too much on reducing the background.

order one couplings) and the maximum final-state center-of-mass energy can be achieved without large penalties on the reach. With b-tagging, one is also able to pick out and probe the b-quark related operators with a reasonable sensitivity. Precise estimations for the signal rates as well as background estimation is crucial for a more realistic projection for the reach of the $\gamma q \to \gamma q$ channel. Our study then provides additional motivations for such estimations to be done in the future.

With the forward proton tagger it is possible to explore a wider class of processes that are sensitive to other dim-8 operators. Another process of interest is $\gamma\gamma \to WW/ZZ$, with its result usually interpreted in terms of bounds on dim-6 and dim-8 anomalous quartic gauge couplings. The analysis by the CMS and TOTEM collaborations [45] reported the reach on several dim-6 and dim-8 operator coefficients, some of which already at the TeV-scale level (assuming order-one couplings). It is however challenging to separate the dim-6 and dim-8 effects, as well as the different dim-8 contributions in these channels, which makes the interpretation of positivity bounds less trivial. On the other hand, for the light-by-light process, $\gamma\gamma \to \gamma\gamma$, the leading new physics contributions also come as dim-8 operators. However, the SM contribution to this process is highly suppressed, so the leading BSM contribution is in the dim-8-squared term. The search for this process has been done in the CMS and TOTEM analyses [46] (see e.g. ref. [53] for similar measurements in nuclei collisions), and the null results were interpreted as the bounds on the coefficients of dim-8 operators $(F_{\mu\nu}F^{\mu\nu})^2$ and $\left(F_{\mu\nu}\widetilde{F}^{\mu\nu}\right)^2$. Since the measurements are only sensitive to the dim-8-squared term, these results unfortunately do not offer a probe on the positivity bounds.

Acknowledgments

A Positivity bounds for dim-8 operators

The $f^+ f^- \gamma^+ \gamma^-$ 4-point amplitude, where $f = e_{L,R}$ and $\pm$ denotes the sign of helicities, is given by [14]

$$\mathcal{A}\left(f^+ f^- \gamma^+ \gamma^-\right)_{\text{SM+dim-8}} = 2e^2 \frac{\langle 24 \rangle^2}{\langle 13 \rangle \langle 23 \rangle} + \frac{a}{v^4}[13][23]\langle 24 \rangle^2$$

$$= 2e^2 \frac{\langle 24 \rangle^2}{\langle 13 \rangle \langle 23 \rangle}\left(1 + \frac{a}{2e^2 v^4}tu\right), \tag{A.1}$$

where a is the (dimensionless) Wilson coefficient of the contact dim-8 operator, normalized by v^4. To go from this amplitude to the one of interest in our paper, $\mathcal{A}\left(\gamma^+ \gamma^- f^+ f^-\right)$, one

simply make the exchange $1 \leftrightarrow 2$ and $3 \leftrightarrow 4$ for the spinor brackets. They are also related to the elastic amplitude $\mathcal{A}\left(f^+\gamma^+f^-\gamma^-\right)$ by crossing, which is given by

$$\mathcal{A}\left(f^+\gamma^+f^-\gamma^-\right)_{\text{SM+dim-8}} = 2e^2 \frac{\langle 34\rangle^2}{\langle 12\rangle\langle 32\rangle}\left(1 + \frac{a}{2e^2v^4}su\right) \xrightarrow{t\to 0} -2e^2\left(1 - \frac{a}{2e^2v^4}s^2\right),$$
(A.2)

where the last step gives the amplitude in the forward limit, $t \to 0$. The positivity bound, $\frac{d^2}{ds^2}\mathcal{A}(f^+\gamma^+f^-\gamma^-)|_{t\to 0} \geq 0$, implies $a \geq 0$. We denote the a parameter by a_L and a_R for $f = e_L$ and $f = e_R$, respectively. They are related to the dim-8 operator coefficients by

$$a_L = -2\frac{v^4}{\Lambda^4}\left(c_W^2 c_{l^2B^2D} - 2s_Wc_W c_{l^2WBD}^{(2)} + s_W^2 c_{l^2W^2D}^{(1)}\right),$$
$$a_R = -2\frac{v^4}{\Lambda^4}\left(c_W^2 c_{e^2B^2D} + s_W^2 c_{e^2W^2D}\right).$$
(A.3)

where the dim-8 Lagrangian is written as $\mathcal{L}_{\text{dim-8}} = \sum_i \frac{c_i}{\Lambda^4}Q_i$ and the corresponding operators Q_i are given by [85, 86]

$$\begin{aligned}
Q_{l^2B^2D} &= i\left(\bar{l}\gamma^\mu \overleftrightarrow{D}^\nu l\right)B_{\mu\rho}B_\nu{}^\rho, \\
Q_{l^2WBD}^{(2)} &= i\left(\bar{l}\gamma^\mu\tau^I\overleftrightarrow{D}^\nu l\right)\left(B_{\mu\rho}W_\nu^{I\rho} + B_{\nu\rho}W_\mu^{I\rho}\right), \\
Q_{l^2W^2D}^{(1)} &= i\left(\bar{l}\gamma^\mu \overleftrightarrow{D}^\nu l\right)W_{\mu\rho}^I W_\nu^{I\rho}, \\
Q_{e^2B^2D} &= i\left(\bar{e}\gamma^\mu \overleftrightarrow{D}^\nu e\right)B_{\mu\rho}B_\nu{}^\rho, \\
Q_{e^2W^2D} &= i\left(\bar{e}\gamma^\mu \overleftrightarrow{D}^\nu e\right)W_{\mu\rho}^I W_\nu^{I\rho}.
\end{aligned}$$
(A.4)

Open Access. This article is distributed under the terms of the Creative Commons Attribution License (CC-BY4.0), which permits any use, distribution and reproduction in any medium, provided the original author(s) and source are credited.

References

[1] A. Adams, N. Arkani-Hamed, S. Dubovsky, A. Nicolis and R. Rattazzi, *Causality, analyticity and an IR obstruction to UV completion*, *JHEP* **10** (2006) 014 [hep-th/0602178] [INSPIRE].

[2] B. Bellazzini, *Softness and amplitudes' positivity for spinning particles*, *JHEP* **02** (2017) 034 [arXiv:1605.06111] [INSPIRE].

[3] B. Bellazzini, F. Riva, J. Serra and F. Sgarlata, *The other effective fermion compositeness*, *JHEP* **11** (2017) 020 [arXiv:1706.03070] [INSPIRE].

[4] C. de Rham, S. Melville, A.J. Tolley and S.-Y. Zhou, *Positivity bounds for scalar field theories*, *Phys. Rev. D* **96** (2017) 081702 [arXiv:1702.06134] [INSPIRE].

[5] C. de Rham, S. Melville, A.J. Tolley and S.-Y. Zhou, *UV complete me: Positivity Bounds for Particles with Spin*, *JHEP* **03** (2018) 011 [arXiv:1706.02712] [INSPIRE].

[6] C. de Rham, S. Melville, A.J. Tolley and S.-Y. Zhou, *Positivity Bounds for Massive Spin-1 and Spin-2 Fields*, *JHEP* **03** (2019) 182 [arXiv:1804.10624] [INSPIRE].

[7] B. Bellazzini and F. Riva, *New phenomenological and theoretical perspective on anomalous ZZ and Zγ processes*, *Phys. Rev. D* **98** (2018) 095021 [arXiv:1806.09640] [INSPIRE].

[8] Q. Bi, C. Zhang and S.-Y. Zhou, *Positivity constraints on aQGC: carving out the physical parameter space*, *JHEP* **06** (2019) 137 [arXiv:1902.08977] [INSPIRE].

[9] G.N. Remmen and N.L. Rodd, *Consistency of the Standard Model Effective Field Theory*, *JHEP* **12** (2019) 032 [arXiv:1908.09845] [INSPIRE].

[10] G.N. Remmen and N.L. Rodd, *Flavor Constraints from Unitarity and Analyticity*, *Phys. Rev. Lett.* **125** (2020) 081601 [*Erratum ibid.* **127** (2021) 149901] [arXiv:2004.02885] [INSPIRE].

[11] C. Zhang and S.-Y. Zhou, *Convex Geometry Perspective on the (Standard Model) Effective Field Theory Space*, *Phys. Rev. Lett.* **125** (2020) 201601 [arXiv:2005.03047] [INSPIRE].

[12] B. Fuks, Y. Liu, C. Zhang and S.-Y. Zhou, *Positivity in electron-positron scattering: testing the axiomatic quantum field theory principles and probing the existence of UV states*, *Chin. Phys. C* **45** (2021) 023108 [arXiv:2009.02212] [INSPIRE].

[13] K. Yamashita, C. Zhang and S.-Y. Zhou, *Elastic positivity vs. extremal positivity bounds in SMEFT: a case study in transversal electroweak gauge-boson scatterings*, *JHEP* **01** (2021) 095 [arXiv:2009.04490] [INSPIRE].

[14] J. Gu, L.-T. Wang and C. Zhang, *Unambiguously Testing Positivity at Lepton Colliders*, *Phys. Rev. Lett.* **129** (2022) 011805 [arXiv:2011.03055] [INSPIRE].

[15] T. Trott, *Causality, unitarity and symmetry in effective field theory*, *JHEP* **07** (2021) 143 [arXiv:2011.10058] [INSPIRE].

[16] Q. Bonnefoy, E. Gendy and C. Grojean, *Positivity bounds on Minimal Flavor Violation*, *JHEP* **04** (2021) 115 [arXiv:2011.12855] [INSPIRE].

[17] M. Chala and J. Santiago, *Positivity bounds in the standard model effective field theory beyond tree level*, *Phys. Rev. D* **105** (2022) L111901 [arXiv:2110.01624] [INSPIRE].

[18] C. Zhang, *SMEFTs living on the edge: determining the UV theories from positivity and extremality*, *JHEP* **12** (2022) 096 [arXiv:2112.11665] [INSPIRE].

[19] X. Li and S. Zhou, *Origin of neutrino masses on the convex cone of positivity bounds*, *Phys. Rev. D* **107** (2023) L031902 [arXiv:2202.12907] [INSPIRE].

[20] C. de Rham, S. Kundu, M. Reece, A.J. Tolley and S.-Y. Zhou, *Snowmass White Paper: UV Constraints on IR Physics*, in the proceedings of the *Snowmass 2021*, Seattle, U.S.A., 17–26 July 2022, arXiv:2203.06805 [INSPIRE].

[21] X. Li, K. Mimasu, K. Yamashita, C. Yang, C. Zhang and S.-Y. Zhou, *Moments for positivity: using Drell-Yan data to test positivity bounds and reverse-engineer new physics*, *JHEP* **10** (2022) 107 [arXiv:2204.13121] [INSPIRE].

[22] S. Hamoudou, J. Kumar and D. London, *Dimension-8 SMEFT matching conditions for the low-energy effective field theory*, *JHEP* **03** (2023) 157 [arXiv:2207.08856] [INSPIRE].

[23] X. Li, *Positivity bounds at one-loop level: the Higgs sector*, *JHEP* **05** (2023) 230 [arXiv:2212.12227] [INSPIRE].

[24] M. Chala, *Constraints on anomalous dimensions from the positivity of the S matrix*, *Phys. Rev. D* **108** (2023) 015031 [arXiv:2301.09995] [INSPIRE].

[25] J. Davighi, S. Melville, K. Mimasu and T. You, *Positivity and the electroweak hierarchy*, *Phys. Rev. D* **109** (2024) 033009 [arXiv:2308.06226] [INSPIRE].

[26] Q. Chen, K. Mimasu, T.A. Wu, G.-D. Zhang and S.-Y. Zhou, *Capping the positivity cone: dimension-*8 *Higgs operators in the SMEFT*, *JHEP* **03** (2024) 180 [arXiv:2309.15922] [INSPIRE].

[27] M. Chala and X. Li, *Positivity restrictions on the mixing of dimension-eight SMEFT operators*, *Phys. Rev. D* **109** (2024) 065015 [arXiv:2309.16611] [INSPIRE].

[28] I. Low, R. Rattazzi and A. Vichi, *Theoretical Constraints on the Higgs Effective Couplings*, *JHEP* **04** (2010) 126 [arXiv:0907.5413] [INSPIRE].

[29] A. Falkowski, S. Rychkov and A. Urbano, *What if the Higgs couplings to W and Z bosons are larger than in the Standard Model?*, *JHEP* **04** (2012) 073 [arXiv:1202.1532] [INSPIRE].

[30] B. Bellazzini, L. Martucci and R. Torre, *Symmetries, Sum Rules and Constraints on Effective Field Theories*, *JHEP* **09** (2014) 100 [arXiv:1405.2960] [INSPIRE].

[31] J. Gu and L.-T. Wang, *Sum Rules in the Standard Model Effective Field Theory from Helicity Amplitudes*, *JHEP* **03** (2021) 149 [arXiv:2008.07551] [INSPIRE].

[32] A. Azatov, D. Ghosh and A.H. Singh, *Four-fermion operators at dimension* 6*: Dispersion relations and UV completions*, *Phys. Rev. D* **105** (2022) 115019 [arXiv:2112.02302] [INSPIRE].

[33] G.N. Remmen and N.L. Rodd, *Signs, spin, SMEFT: Sum rules at dimension six*, *Phys. Rev. D* **105** (2022) 036006 [arXiv:2010.04723] [INSPIRE].

[34] G.N. Remmen and N.L. Rodd, *Spinning sum rules for the dimension-six SMEFT*, *JHEP* **09** (2022) 030 [arXiv:2206.13524] [INSPIRE].

[35] J. Davighi, S. Melville and T. You, *Natural selection rules: new positivity bounds for massive spinning particles*, *JHEP* **02** (2022) 167 [arXiv:2108.06334] [INSPIRE].

[36] W. Altmannshofer, S. Gori, B.V. Lehmann and J. Zuo, *UV physics from IR features: New prospects from top flavor violation*, *Phys. Rev. D* **107** (2023) 095025 [arXiv:2303.00781] [INSPIRE].

[37] J. Ellis, S.-F. Ge, H.-J. He and R.-Q. Xiao, *Probing the scale of new physics in the $ZZ\gamma$ coupling at e^+e^- colliders*, *Chin. Phys. C* **44** (2020) 063106 [arXiv:1902.06631] [INSPIRE].

[38] J. Ellis, H.-J. He and R.-Q. Xiao, *Probing new physics in dimension-*8 *neutral gauge couplings at e^+e^- colliders*, *Sci. China Phys. Mech. Astron.* **64** (2021) 221062 [arXiv:2008.04298] [INSPIRE].

[39] S. Alioli, R. Boughezal, E. Mereghetti and F. Petriello, *Novel angular dependence in Drell-Yan lepton production via dimension-*8 *operators*, *Phys. Lett. B* **809** (2020) 135703 [arXiv:2003.11615] [INSPIRE].

[40] J. Ellis, H.-J. He and R.-Q. Xiao, *Probing neutral triple gauge couplings at the LHC and future hadron colliders*, *Phys. Rev. D* **107** (2023) 035005 [arXiv:2206.11676] [INSPIRE].

[41] J. Ellis, H.-J. He and R.-Q. Xiao, *Probing neutral triple gauge couplings with $Z^*\gamma\,(\nu\bar{\nu}\gamma)$ production at hadron colliders*, *Phys. Rev. D* **108** (2023) L111704 [arXiv:2308.16887] [INSPIRE].

[42] ATLAS collaboration, *Measurement of the exclusive $\gamma\gamma \to \mu^+\mu^-$ process in proton-proton collisions at $\sqrt{s} = 13$ TeV with the ATLAS detector*, *Phys. Lett. B* **777** (2018) 303 [arXiv:1708.04053] [INSPIRE].

[43] ATLAS collaboration, *Observation and Measurement of Forward Proton Scattering in Association with Lepton Pairs Produced via the Photon Fusion Mechanism at ATLAS*, *Phys. Rev. Lett.* **125** (2020) 261801 [arXiv:2009.14537] [INSPIRE].

[44] ATLAS collaboration, *Observation of photon-induced W^+W^- production in pp collisions at* $\sqrt{s} = 13$ *TeV using the ATLAS detector*, *Phys. Lett. B* **816** (2021) 136190 [arXiv:2010.04019] [INSPIRE].

[45] CMS and TOTEM collaborations, *Search for high-mass exclusive* $\gamma\gamma \to WW$ *and* $\gamma\gamma \to ZZ$ *production in proton-proton collisions at* $\sqrt{s} = 13$ *TeV*, *JHEP* **07** (2023) 229 [arXiv:2211.16320] [INSPIRE].

[46] TOTEM and CMS collaborations, *First Search for Exclusive Diphoton Production at High Mass with Tagged Protons in Proton-Proton Collisions at* $\sqrt{s} = 13$ *TeV*, *Phys. Rev. Lett.* **129** (2022) 011801 [arXiv:2110.05916] [INSPIRE].

[47] ATLAS collaboration, *Measurement of exclusive pion pair production in proton-proton collisions at* $\sqrt{s} = 7$ *TeV with the ATLAS detector*, *Eur. Phys. J. C* **83** (2023) 627 [arXiv:2212.00664] [INSPIRE].

[48] L. Adamczyk et al., *Technical Design Report for the ATLAS Forward Proton Detector*, CERN-LHCC-2015-009 (2015).

[49] ATLAS collaboration, *Proton tagging with the one arm AFP detector*, ATL-PHYS-PUB-2017-012 (2017).

[50] M. Albrow et al., *CMS-TOTEM Precision Proton Spectrometer*, CERN-LHCC-2014-021 (2014).

[51] A.J. Baltz, *The Physics of Ultraperipheral Collisions at the LHC*, *Phys. Rep.* **458** (2008) 1 [arXiv:0706.3356] [INSPIRE].

[52] S. Klein and P. Steinberg, *Photonuclear and Two-photon Interactions at High-Energy Nuclear Colliders*, *Annu. Rev. Nucl. Part. Sci.* **70** (2020) 323 [arXiv:2005.01872] [INSPIRE].

[53] ATLAS collaboration, *Measurement of light-by-light scattering and search for axion-like particles with* $2.2\,nb^{-1}$ *of Pb+Pb data with the ATLAS detector*, *JHEP* **03** (2021) 243 [*Erratum ibid.* **11** (2021) 050] [arXiv:2008.05355] [INSPIRE].

[54] ATLAS collaboration, *Exclusive dielectron production in ultraperipheral Pb+Pb collisions at* $\sqrt{s_{\mathrm{NN}}} = 5.02$ *TeV with ATLAS*, *JHEP* **06** (2023) 182 [arXiv:2207.12781] [INSPIRE].

[55] ATLAS collaboration, *Exclusive dilepton production in ultraperipheral Pb+Pb collisions in ATLAS*, *PoS* **LHCP2022** (2023) 313 [INSPIRE].

[56] ATLAS collaboration, *Observation of the* $\gamma\gamma \to \tau\tau$ *Process in Pb+Pb Collisions and Constraints on the* τ-*Lepton Anomalous Magnetic Moment with the ATLAS Detector*, *Phys. Rev. Lett.* **131** (2023) 151802 [arXiv:2204.13478] [INSPIRE].

[57] M. Demirci and M.F. Mustamin, *One-loop electroweak radiative corrections to charged lepton pair production in photon-photon collisions*, *Phys. Rev. D* **103** (2021) 113004 [arXiv:2105.05340] [INSPIRE].

[58] D.Y. Shao, C. Zhang, J. Zhou and Y.-J. Zhou, *Azimuthal asymmetries of muon pair production in ultraperipheral heavy ion collisions*, *Phys. Rev. D* **107** (2023) 036020 [arXiv:2212.05775] [INSPIRE].

[59] D.Y. Shao, C. Zhang, J. Zhou and Y.-J. Zhou, *Lepton pair production in ultraperipheral collisions: Toward a precision test of the resummation formalism*, *Phys. Rev. D* **108** (2023) 116015 [arXiv:2306.02337] [INSPIRE].

[60] D.Y. Shao, B. Yan, S.-R. Yuan and C. Zhang, *Spin asymmetry and dipole moments in* τ-*pair production with ultraperipheral heavy ion collisions*, arXiv:2310.14153 [INSPIRE].

[61] H.-S. Shao and D. d'Enterria, *gamma-UPC: automated generation of exclusive photon-photon processes in ultraperipheral proton and nuclear collisions with varying form factors*, *JHEP* **09** (2022) 248 [arXiv:2207.03012] [INSPIRE].

[62] MUON $g-2$ collaboration, *Final Report of the Muon E821 Anomalous Magnetic Moment Measurement at BNL*, *Phys. Rev. D* **73** (2006) 072003 [hep-ex/0602035] [INSPIRE].

[63] MUON $g-2$ collaboration, *An Improved Limit on the Muon Electric Dipole Moment*, *Phys. Rev. D* **80** (2009) 052008 [arXiv:0811.1207] [INSPIRE].

[64] ACME collaboration, *Improved limit on the electric dipole moment of the electron*, *Nature* **562** (2018) 355 [INSPIRE].

[65] MUON $g-2$ collaboration, *Measurement of the Positive Muon Anomalous Magnetic Moment to* 0.46 *ppm*, *Phys. Rev. Lett.* **126** (2021) 141801 [arXiv:2104.03281] [INSPIRE].

[66] J. Baglio, S. Dawson and I.M. Lewis, *NLO effects in EFT fits to W^+W^- production at the LHC*, *Phys. Rev. D* **99** (2019) 035029 [arXiv:1812.00214] [INSPIRE].

[67] P. Azzi et al., *Report from Working Group 1: Standard Model Physics at the HL-LHC and HE-LHC*, *CERN Yellow Reports: Monographs* **7** (2019) 1 [arXiv:1902.04070] [INSPIRE].

[68] S. Klein, A.H. Mueller, B.-W. Xiao and F. Yuan, *Lepton Pair Production Through Two Photon Process in Heavy Ion Collisions*, *Phys. Rev. D* **102** (2020) 094013 [arXiv:2003.02947] [INSPIRE].

[69] M. Kłusek-Gawenda, W. Schäfer and A. Szczurek, *Centrality dependence of dilepton production via $\gamma\gamma$ processes from Wigner distributions of photons in nuclei*, *Phys. Lett. B* **814** (2021) 136114 [arXiv:2012.11973] [INSPIRE].

[70] R.-j. Wang, S. Pu and Q. Wang, *Lepton pair production in ultraperipheral collisions*, *Phys. Rev. D* **104** (2021) 056011 [arXiv:2106.05462] [INSPIRE].

[71] R.-j. Wang, S. Lin, S. Pu, Y.-f. Zhang and Q. Wang, *Lepton pair photoproduction in peripheral relativistic heavy-ion collisions*, *Phys. Rev. D* **106** (2022) 034025 [arXiv:2204.02761] [INSPIRE].

[72] X. Wang et al., *Collision-energy dependence of the Breit-Wheeler process in heavy-ion collisions and its application to nuclear charge radius measurements*, *Phys. Rev. C* **107** (2023) 044906 [arXiv:2207.05595] [INSPIRE].

[73] J. Alwall et al., *The automated computation of tree-level and next-to-leading order differential cross sections, and their matching to parton shower simulations*, *JHEP* **07** (2014) 079 [arXiv:1405.0301] [INSPIRE].

[74] CEPC STUDY Group, *CEPC Conceptual Design Report: Volume 2 — Physics & Detector*, arXiv:1811.10545 [INSPIRE].

[75] FCC collaboration, *FCC-ee: The Lepton Collider: Future Circular Collider Conceptual Design Report Volume 2*, *Eur. Phys. J. Spec. Top.* **228** (2019) 261 [INSPIRE].

[76] P. Bambade et al., *The International Linear Collider: A Global Project*, arXiv:1903.01629 [INSPIRE].

[77] CEPC PHYSICS STUDY Group, *The Physics potential of the CEPC. Prepared for the U.S. Snowmass Community Planning Exercise (Snowmass 2021)*, in the proceedings of the *Snowmass 2021*, Seattle, U.S.A., 17–26 July 2022, arXiv:2205.08553 [INSPIRE].

[78] R. Contino, A. Falkowski, F. Goertz, C. Grojean and F. Riva, *On the Validity of the Effective Field Theory Approach to SM Precision Tests*, *JHEP* **07** (2016) 144 [arXiv:1604.06444] [INSPIRE].

[79] S. Alte, M. König and W. Shepherd, *Consistent Searches for SMEFT Effects in Non-Resonant Dijet Events*, *JHEP* **01** (2018) 094 [arXiv:1711.07484] [INSPIRE].

[80] R. Bruce et al., *HL-LHC operational scenarios for Pb-Pb and p-Pb operation*, CERN-ACC-2020-0011 (2020).

[81] Z. Liu, K.-F. Lyu and T. Wu, *LHC Shine Lights on Positivity*, in progress.

[82] A. Manohar, P. Nason, G.P. Salam and G. Zanderighi, *How bright is the proton? A precise determination of the photon parton distribution function*, *Phys. Rev. Lett.* **117** (2016) 242002 [arXiv:1607.04266] [INSPIRE].

[83] Y. Hatta, B.-W. Xiao and F. Yuan, *Semi-inclusive diffractive deep inelastic scattering at small x*, *Phys. Rev. D* **106** (2022) 094015 [arXiv:2205.08060] [INSPIRE].

[84] L.A. Harland-Lang, A.D. Martin, P. Motylinski and R.S. Thorne, *Parton distributions in the LHC era: MMHT 2014 PDFs*, *Eur. Phys. J. C* **75** (2015) 204 [arXiv:1412.3989] [INSPIRE].

[85] C.W. Murphy, *Dimension-8 operators in the Standard Model Eective Field Theory*, *JHEP* **10** (2020) 174 [arXiv:2005.00059] [INSPIRE].

[86] H.-L. Li, Z. Ren, J. Shu, M.-L. Xiao, J.-H. Yu and Y.-H. Zheng, *Complete set of dimension-eight operators in the standard model effective field theory*, *Phys. Rev. D* **104** (2021) 015026 [arXiv:2005.00008] [INSPIRE].